Seeing a single photon without destroying it

G. Nogues, A. Rauschenbeutel, S. Osnaghi, M. Brune, J. M. Raimond & S. Haroche

Laboratoire Kastler Brossel, Département de Physique de l'Ecole Normale Supérieure, 24 rue Lhomond, F-75231, Paris Cedex 05, France

Light detection is usually a destructive process, in that detectors annihilate photons and convert them into electrical signals, making it impossible to see a single photon twice. But this limitation is not fundamental—quantum non-demolition strategies[1–3] permit repeated measurements of physically observable quantities, yielding identical results. For example, quantum non-demolition measurements of light intensity have been demonstrated[4–14], suggesting possibilities for detecting weak forces and gravitational waves[3]. But such experiments, based on nonlinear optics, are sensitive only to macroscopic photon fluxes. The non-destructive measurement of a single photon requires an extremely strong matter–radiation coupling; this can be realized in cavity quantum electrodynamics[15], where the strength of the interaction between an atom and a photon can overwhelm all dissipative couplings to the environment. Here we report a cavity quantum electrodynamics experiment in which we detect a single photon non-destructively. We use atomic interferometry to measure the phase shift in an atomic wavefunction, caused by a cycle of photon absorption and emission. Our method amounts to a restricted quantum non-demolition measurement which can be applied only to states containing one or zero photons. It may lead to quantum logic gates[16] based on cavity quantum electrodynamics, and multi-atom entanglement[17].

In optical quantum non-demolition (QND) measurements, a 'signal' beam is coupled to a 'meter' beam in a nonlinear medium whose refractive index depends on light intensity[4]. The phase shift of the meter resulting from the non-resonant couplings of the beams with the medium is measured by optical interferometry. The meter beam is split into two parts, one of which is coupled to the signal, the other being used as reference. The two parts are recombined before reading the meter output intensity. The signal intensity remains unaltered. In the single-photon quantum non-demolition (SP-QND) scheme described here, this procedure is modified by replacing the meter light beam with a single atom interacting resonantly with the signal field and by resorting to atomic instead of optical interferometry.

The signal field is now stored in a mode of a cavity C (Fig. 1a). Meter atoms cross C one at a time. The relevant atomic levels (e, g and i) are shown in the inset of Fig. 1a. The cavity field is resonant with the e ⇒ g transition, while i is a reference level (the g ⇒ i transition is non-resonant with C). Let us first assume that there is 1 photon in C and that the meter enters C in level g at time $t = 0$. As the meter crosses C, the combined atom–field system undergoes a reversible Rabi oscillation[18] at angular frequency Ω between the states $|g,1\rangle$ and $|e,0\rangle$ representing respectively the meter in g or e with 1 or 0 photon in C. At time t, the system is in the coherent superposition: $\cos(\Omega t/2)|g,1\rangle + \sin(\Omega t/2)|e,0\rangle$.

If the total interaction time is $2\pi/\Omega$ (2π Rabi pulse), the atom ends up in g after a full coherent cycle of photon absorption and emission and the photon number is left unchanged. The system has, however, experienced a subtle quantum alteration. The global phase of the state has changed, $|g,1\rangle$ turning into $-|g,1\rangle = e^{i\pi}|g,1\rangle$. A similar π phase shift occurs when performing a 2π rotation on a spin-1/2 particle[19,20]. Alternatively, if C is empty, or if the atom crosses C in i, the system's state remains unaltered. As a result, a state superposition $C_g|g,1\rangle + C_i|i,1\rangle$ is transformed into $C_g e^{i\pi}|g,1\rangle + C_i|i,1\rangle$ while, in the empty-cavity case, $C_g|g,0\rangle + C_i|i,0\rangle$ is unchanged. In short, the atomic coherence changes its phase by π if there is 1 photon in C.

The meter wavefunction phase-shift is measured by Ramsey interferometry[21]. The meter, initially in g, undergoes two interactions with a classical auxiliary field (frequency ν), before and after crossing the cavity mode (zones R_1 and R_2 in Fig. 1a). This field is nearly resonant with the g ⇒ i transition at frequency ν_{gi}. The first pulse prepares the coherent superposition $(1/\sqrt{2})(|g\rangle + |i\rangle)$ and the second mixes the states again, probing after C the superposition phase-shift. The final atomic populations are measured downstream with a state-selective detector D. The probability of finding the meter in g or i results from a quantum interference between two paths in which the atom crosses C in either g or i. It is modulated when ν is tuned, resulting in sinusoidal 'Ramsey fringes'.

When C contains 1 photon, the amplitude associated with one of the paths (atom in g) is phase-shifted by π. The corresponding fringe pattern should thus be π out of phase with the one obtained with C empty. The interfering quantum paths and the corresponding fringes are depicted in Fig. 1b,c. Setting ν at a fringe extremum (for instance at $\nu - \nu_{gi} = 0$) results in a perfect correlation between the state of the meter (i or g) and the photon number (0 or 1).

This SP-QND scheme can measure only two photon numbers (0 and 1) in a non-demolition way. For an n-photon field with $n > 1$, the Rabi frequency is $\Omega\sqrt{n}$ and n-conservation cannot be enforced for all ns. By slightly detuning the cavity from the e ⇒ g transition, it is however possible to suppress the meter absorption, thus avoiding completely photon demolition. The dispersive phase shift experienced by the meter in the non-resonant case is dependent upon the photon number. This shift could also be measured by Ramsey interferometry, leading now to an unrestricted QND measurement of the photon number. This dispersive method was described in our original cavity quantum electrodynamics-quantum

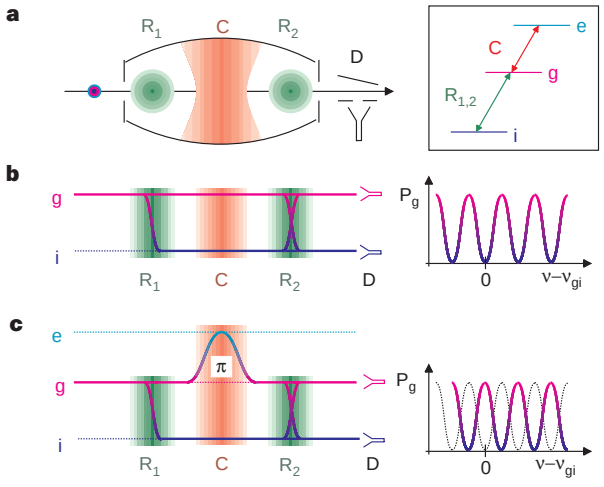

Figure 1 Scheme of our atom interferometer, which can detect single photons. **a,** Atoms cross the cavity C one at a time; the cavity mode (shown in red) stores the field to be measured. The e, g and i atomic levels are shown in the inset. The cavity mode is resonant with the e ⇒ g transition. Atoms are subjected in zones R_1 and R_2 (in green) to auxiliary pulses (frequency ν), quasi-resonant with the g ⇒ i transition (frequency ν_{gi}). Detector D, downstream, measures the states of the atoms. **b,** Diagram depicting the interfering paths followed by an atom initially in g when there is no photon in the cavity mode. The atom travels between R_1 and R_2 either in g (violet line) or in i (blue line). The probability amplitudes associated with these two paths interfere, leading to fringes in the probability P_g of detecting the atom in g when ν is scanned (shown at right). **c,** As **b** but when the cavity mode stores one photon. The atom, if in level g, undergoes a full reversible cycle of photon absorption and emission, finally leaving the photon in C. In the process, the corresponding amplitude has undergone a π phase shift and the fringes are reversed (as shown at right).

non-demolition proposal[22,23]. It is, however, more difficult to implement than the resonant SP-QND scheme described here as it corresponds to a smaller phase-shift per photon for a given atom–cavity interaction time. We note that a SP-QND measurement based on a 2π Rabi pulse has already been suggested[24]. It relied, however, on the observation of a deflection of the atomic trajectory and not on an interference effect as discussed here. Note also that multiples of 2π Rabi pulses leaving the photon number unchanged are essential to generate "trapping states"[25] in a micromaser.

In our set-up[26–28], a thermal beam of rubidium atoms is velocity-selected by laser-induced optical pumping. The atoms are then prepared in the Rydberg circular state with principal quantum number 50 (level g) or 51 (level e). The e ⇒ g transition is resonant at 51.1 GHz. Circular Rydberg states[29,30] have exceptionally large coupling to microwave radiation and long lifetimes (~30 ms for e and g), two essential features here. The circular state preparation[30] is pulsed. It generates at a pre-set time (within ±1 μs) an atomic sample with, on average, 0.3–0.6 atom. In most samples, there is zero or one atom present. This time-resolved process, combined with velocity selection, determines the atomic position at any time within ±1 mm.

Each atom crosses the apparatus before entering a state-selective field-ionization detector D (efficiency, 30%). The interferometer operates on the 54.3-GHz g ⇒ i transition (i is the circular state with principal quantum number 49). The set-up is cooled to 0.6 or 1.2 K by a helium cryostat. The average number of thermal photons in the mode at these temperatures are 0.02 and 0.15, respectively. The cavity is made of two niobium spherical mirrors in a Fabry–Perot configuration. The mirrors are surrounded by a cylindrical ring (with 3-mm holes for atom access) which reflects the photons scattered by the imperfections of the mirrors back into the cavity mode, thus reducing its losses. The resulting photon decay time is 1 ms, long enough to permit repeated field measurements.

The cavity sustains a transverse electromagnetic gaussian mode (waist w=6 mm), resonant with the e ⇒ g transition. The single-photon Rabi frequency at cavity centre is $\Omega/2\pi$=47 kHz (ref. 18). The atomic velocity, V=503(±2.5) m s^{-1}, corresponds to an effective interaction time $t_i = \sqrt{\pi}\, w/V$ such that $\Omega t_i = 2\pi$. A small electric field is applied across the two electrically isolated mirrors. This field is used to fine-tune the atomic frequency through the Stark effect. By commuting it at pre-set times, the e ⇒ g transition can be put in or out of resonance with C, allowing us to reduce to a fraction of t_i the atom–cavity interaction time (see below).

The stray electric fields across the ring holes prevent atomic coherence from propagating in and out of C. We thus apply the Ramsey pulses inside the closed cavity structure, by injecting the 54.3-GHz radiation through an additional hole in the ring. This radiation does not couple with the 51.1-GHz mode. It produces a standing-wave pattern, mapped by performing time-resolved spectroscopy of the Rydberg states. This standing-wave exhibits two field antinodes sandwiching the cavity mode waist (R_1 and R_2 in Fig. 1a). As we know the position of each atom as a function of time, we can apply controlled pulses when the meter crosses R_1 and R_2. The resulting fringes, detected by accumulating statistics of atom counts in g and i, have a 72% contrast (g and i states probabilities oscillating between 0.86 and 0.14).

An experimental sequence consists of preparing a small field in C, then measuring it by sending a meter atom across the interferometer, possibly checking the result with another atom. Statistics are accumulated over an ensemble of sequences. Since each atom sample has a 0.1–0.2 probability of yielding a signal, the probability of detecting an atom pair is only 1–4%. To limit data acquisition time, sequences are repeated after 1.5 ms, without waiting for complete cavity relaxation. A photon erasing procedure is used to remove residual photons at the start of each sequence. Photon erasing is also important because the waveguide injecting the Ramsey pulses leaks into C a small thermal field, corresponding to an average of 0.7 photons (this value is deduced from a measurement of the g ⇒ e absorption rate of an atom crossing C). Each sequence starts by sending five pulses of atoms prepared in g. These eraser pulses contain three to nine atoms each. They absorb the remaining field, cooling the mode down to 0.12 photons on average. The experimental sequence is then performed within 400 μs, to limit thermal field build-up.

In a first experiment, we use a source atom to generate a single photon[28]. This atom, prepared in e, is sent across C, 100 μs after the last eraser pulse. The interaction time of the source with the mode is reduced to $t_i/4$ by Stark-tuning the e ⇒ g transition while the atom is in C. The atom–field system undergoes a $\pi/2$ Rabi pulse and is prepared in the entangled state $(1/\sqrt{2})(|e,0\rangle+|g,1\rangle)$. Detecting the source in e (g) ideally reduces the field to a 0 (1)-photon state. We thus prepare, with equal probabilities, either 0 or 1 photon.

We then send the meter after a 100-μs delay. The interaction time is reset to the value t_i. The 2π Rabi pulse is slightly imperfect, with a 20% residual probability for the meter to absorb the photon. The conditional probabilities $P_{g2/e1}(\nu)$ and $P_{g2/g1}(\nu)$ to detect the meter in g, provided the source has been detected in e or g respectively, are reconstructed as a function of the Ramsey frequency ν. About 250 events are sampled per frequency step. Ideally, these probabilities are equal to the conditional probabilities $P_{g/0}(\nu)$ and $P_{g/1}(\nu)$ of detecting the meter in g if there is 0 or 1 photon in C.

As expected, we obtain two sinusoidal fringe patterns, π phase-shifted with respect to each other (Fig. 2). The fringes corresponding to the source detected in e have the same phase as the ones obtained with C empty. Their contrast is limited to 41% by various known imperfections (see Fig. 2 legend). The lines in the figure result from a simulation taking these imperfections into account. The agreement with the experiment is very good, meaning that the limitations of the apparatus are well understood.

The CQED interferometer is characterized by the sinusoidally varying conditional probabilities $P_{a/0}(\nu)$ and $P_{a/1}(\nu)$, where a stands for g or i. In a practical measurement, the photon number is initially unknown and we are interested in the reverse conditional probabilities

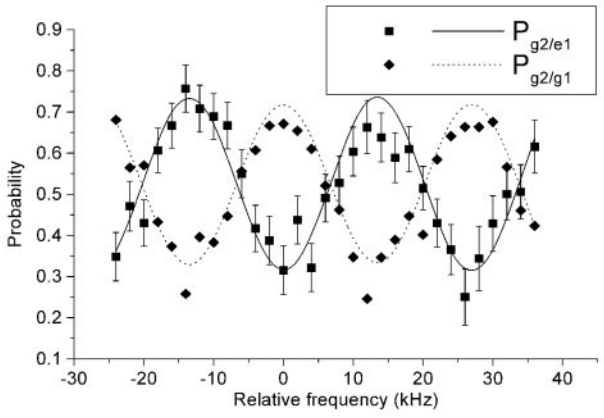

Figure 2 Preparing and detecting one photon. A first atom prepares 0 or 1 photon and a second atom performs an interferometric measurement: recordings of the conditional probabilities $P_{g2/e1}(\nu)$ (squares) and $P_{g2/g1}(\nu)$ (diamonds) of detecting the second atom in g provided the first has been found in e or g (leaving 0 or 1 photon in C). These probabilities are reconstructed as a function of ν by averaging 250 correlated atom counts for each ν value (experimental points; statistical error bars are shown only for $P_{g2/e1}(\nu)$ for the sake of clarity). The two signals, π phase shifted with respect to each other, demonstrate the operation of the single photon sensitive interferometer. The lines result from numerical simulation considering known apparatus imperfections: 72% contrast of the Ramsey interferometer, imperfections of the $\pi/2$ and 2π Rabi pulses, detection errors, samples containing two atoms, residual thermal field in C, and field relaxation between source and meter.

$P_{1/a}(\nu)$ and $P_{0/a}(\nu)$ of having 0 or 1 photon in C after the meter has been found in a given state. A simple application of Bayes laws yields:

$$P_{1/a}(\nu) = P_1.P_{a/1}(\nu)/[P_1.P_{a/1}(\nu) + P_0.P_{a/0}(\nu)] \quad (1)$$

where P_0 and P_1 are the probabilities of having, before measurement, respectively 0 and 1 photon in C (other photon numbers are outside the range of the SP-QND scheme). Equation (1) describes how the information acquired by the meter reading changes the probability of having 1 photon.

To check the physical content of equation (1), we perform a measurement on a small thermal field (average photon number: 0.30(±0.02)) which builds up in C during a 300-μs delay between the last eraser pulse and the meter. The *a priori* photon number probabilities are $P_0 = 0.77$ and $P_1 = 0.18$, with a negligible probability (0.05) of having more than one photon. Following the meter, we send an absorbing probe atom across C. The probe is prepared in g, 75 μs after the meter, and does not undergo any Ramsey pulse. Its interaction time with C, t_i /2, corresponds to a π Rabi pulse in 1 photon. The probability of detecting the probe in e is hence ideally equal to the probability of finding 1 photon in C after the SP-QND measurement.

Figure 3 shows the measured conditional probabilities $P_{e2/g1}(\nu)$ (squares) and $P_{e2/i1}(\nu)$ (diamonds) of detecting the probe in e, provided the meter is detected in g or i, as a function of ν. We have also recorded the probability P_{e2} of detecting the probe in e, when no meter is sent across C (triangles). The lines in Fig. 3, obtained by a simulation taking into account the imperfections listed in Fig. 2 legend, are in very good agreement with the experiment.

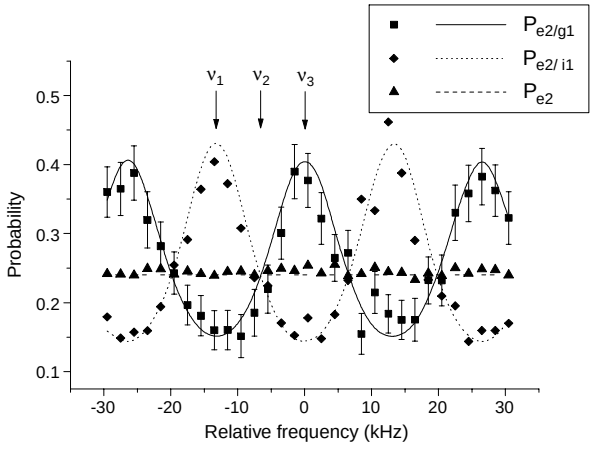

Figure 3 Measuring a photon twice. A first meter atom performs a QND measurement of a small thermal field, and a second probe atom absorbs the field left afterwards. Squares and diamonds indicate experimental points showing the conditional probabilities $P_{e2/g1}(\nu)$ (squares) and $P_{e2/i1}(\nu)$ (diamonds) of finding the probe in e (having absorbed a photon in C), provided that the meter has been measured in g or i. About 650 atom pairs are averaged per frequency step. The probabilities are reconstructed as a function of ν, and the lines are obtained by numerical simulations. The triangles correspond to the probability of finding the probe in e when no measurement is performed on the meter. The periodic variations of the conditional signals show how the information acquired about the field by the first measurement modifies the probability of finding one photon in C. The effect of this measurement depends upon the frequency setting of the interferometer. Three particular frequencies ν_1, ν_2 and ν_3 are indicated by the arrows. At ν_1, 1 photon in C results in a maximum (minimum) probability of finding the meter in i (g). If it is found in i, it is likely that there is 1 photon left in C afterwards. The *a posteriori* probability of finding 1 photon is then larger than the *a priori* probability P_1. The probability that the probe is excited in e exceeds P_{e2} (line of triangles). If the meter is found in g, there is conversely a large probability that C is empty afterwards and the probe excitation probability falls below P_{e2}. At ν_2, the meter indication is ambiguous and the *a posteriori* probe excitation probabilities, equal for both meter states, correspond to the *a priori* probability. At ν_3, level g indicates 1 photon, and the conclusions are opposite to those for ν_1.

The line of triangles represents the average atomic absorption rate of the initial field. The difference between the observed value of P_{e2}, 0.24, and $P_1 = 0.18$ is due to apparatus imperfections. The lines of squares and diamonds show that the probability of having 1 photon in C after reading the meter is either smaller or larger than P_1, depending upon the outcome of the measurement and upon ν (see Fig. 3 legend). The non-demolition feature of the SP-QND measurement is clearly revealed here. When the meter finds 1 photon, it does so without destroying it, leaving it with a high probability behind to excite the probe atom. The detection process by this probe is quite different, as it leaves C empty at the end. The difference between the normal (absorptive) and SP-QND measuring schemes appears clearly here.

We note also that the meter, injected in the lower state of the transition resonant with C, cannot add any energy to the mode. However, detecting it in the state correlated to 1 photon increases the probability of the probe absorbing energy. This might seem paradoxical. In fact, our information about the field (initially described by P_1) is modified by the meter reading (see equation (1)). The change in the probe's absorption rate reflects the fact that we have gained information on the field. Averaging this absorption rate weighted by the respective probabilities of finding the meter in e and g amounts to neglecting the meter information. This average recovers the value corresponding to P_1.

We have also performed a repeated SP-QND measurement, sending two identical meter atoms, 75 μs apart, to detect twice a thermal field with P_1= 0.18. The interferometer was set at frequencies ν_1 and ν_3 (defined in Fig. 2), and, in each case, 1,000 coincidence events were recorded. The conditional probability of finding the second meter in the same state as the first is larger than the *a priori* probability. For example, at ν_1, the *a priori* probability of finding the atom in i is 0.32(±0.01), whereas the conditional probability $P_{i2/i1}$ is increased to the value 0.48 (±0.02). Ideally, these figures should be equal to 0.18 and 1. The observed values are correctly predicted by our numerical model.

We have achieved a single-photon-QND measurement satisfying the criteria of non-demolition and repeatability. Applying our analysis of the interferometer imperfections to the detection of an unknown field containing no more than one photon (P_0=P_1=0.5), we infer that, after a single meter reading, the corresponding photon number probability increases to 0.84. Other developments are in progress. The SP-QND process entangles the 0-1 photon field and the meter. The combined system evolves, before atomic detection, into a coherent superposition of correlated atom–photon states, according to a conditional dynamics in which the photon state controls the atomic state. The SP-QND scheme can be described in terms of quantum logic, and amounts to the operation of a quantum gate[16] in which the photon and the atom play respectively the roles of control and target qubits. By performing a SP-QND measurement of a small coherent field, we are at present studying the coherent operation of this gate. Finally, by allowing us to entangle in a deterministic way several atoms crossing C one at a time, the SP-QND process provides a building block for a general method to entangle an arbitrary number of atoms. A demonstration of three-atom entanglement is under way. □

Received 6 April; accepted 17 May 1999.

1. Braginsky, V. B. & Vorontsov, Y. I. Quantum mechanical limitations in macroscopic experiments and modern experimental techniques. *Usp. Fiz. Nauk.* **114,** 41–53 (1974) [*Sov. Phys. Usp.* **17,** 644–650 (1975)].
2. Braginsky, V. B. & Khalili, F. Y. *Quantum Measurement* (ed. Thorne, K. S.) (Cambridge Univ. Press, 1992).
3. Caves, C. M., Thorne, K. S., Drever, R. W. P., Sandberg, V. D. & Zimmermann, M. On the measurement of a weak classical force coupled to a quantum mechanical oscillator I. Issues of principle. *Rev. Mod. Phys.* **52,** 341–392 (1980).
4. Grangier, P., Levenson, A. L. & Poizat, J. P. Quantum non-demolition measurements in optics. *Nature* **396,** 537–542 (1998).
5. Levenson, M. D., Shelby, R. M., Reid, M. & Walls, D. F. Quantum non-demolition detection of optical quadrature amplitudes. *Phys. Rev. Lett.* **57,** 2473–2476 (1986).
6. La Porta, A., Slusher, R. E. & Yurke, B. Back-action evading measurements of an optical field using parametric down-conversion. *Phys. Rev. Lett.* **62,** 28–31 (1989).

7. Friberg, S. R., Machida, S. & Yamamoto, Y. Quantum non-demolition measurement of the photon number of an optical soliton. *Phys. Rev. Lett.* **69,** 3165–3168 (1992).
8. Roch, J. F., Roger, G., Grangier, P., Courty, J. M. & Reynaud, S. Quantum non-demolition measurements in optics: a review and some recent experimental results. *Appl. Phys. B* **55,** 291–297 (1992).
9. Poizat, J. P. & Grangier P. Experimental realisation of a quantum optical tap. *Phys. Rev. Lett.* **70,** 271–274 (1993).
10. Pereira, S. F., Ou, Z. Y. & Kimble, H. J. Back-action evading measurements for quantum non-demolition detection and quantum optical tapping. *Phys. Rev. Lett.* **72,** 214–217 (1994).
11. Quantum non-demolition measurements. *Appl. Phys. B* **64**(suppl.), 123–272 (1997).
12. Roch, J. F. *et al.* Quantum non-demolition measurements using cold atoms. *Phys. Rev. Lett.* **78,** 634–637 (1997).
13. Bencheick, K., Levenson, J. A., Grangier, P. & Lopez, O. Quantum non-demolition demonstration via repeated back-action evading measurements. *Phys. Rev. Lett.* **75,** 3422–3425 (1995).
14. Bruckmeier, R., Hansen, H. & Schiller, S. Repeated quantum non-demolition measurements of continuous optical waves. *Phys. Rev. Lett.* **79,** 1463–1466 (1997).
15. Haroche, S. & Raimond, J. M. Cavity quantum electrodynamics. *Sci. Am.* **268,** 54–62 (1993).
16. Barenco, A., Deutsch, D. & Ekert, A. Conditional quantum dynamics and logic gates. *Phys. Rev. Lett.* **74,** 4083–4086 (1995).
17. Haroche, S. Atoms and photons in high Q cavities: new tests of quantum theory. *Ann. NY Acad. Sci.* **755,** 73–86 (1995).
18. Brune, M. *et al.* Quantum Rabi oscillation: a direct test of field quantization in a cavity. *Phys. Rev. Lett.* **76,** 1800–1803 (1996).
19. Rauch, H., Zeilinger, A., Badurek, G. & Wilfing, A. Verification of coherent spinor rotation of fermions. *Phys. Lett. A* **54,** 425–427 (1975).
20. Werner, S. A., Colella, R., Overhauser, A. W. & Eagen, C. F. Observation of the phase shift of a neutron due to the precession in a magnetic field. *Phys. Rev. Lett.* **35,** 1053–1055 (1975).
21. Ramsey, N. F. *Molecular Beams* (Oxford Univ. Press, New York, 1985).
22. Brune, M., Haroche, S., Lefèvre, V., Raimond, J. M. & Zagury, N. Quantum non-demolition measurement of small photon numbers by Rydberg atom phase-sensitive detection. *Phys. Rev. Lett.* **65,** 976–979 (1990).
23. Brune, M., Haroche, S., Raimond, J. M., Davidovich, L. & Zagury, N. Manipulation of photons in a cavity by dispersive atom-field coupling: quantum non-demolition measurements and generation of Schrödinger cat states. *Phys. Rev. A* **45,** 5193–5214 (1992).
24. Bragingsky, V. B. & Khalili, F. Ya. Quantum non-demolition measurements: the route from toys to tools. *Rev. Mod. Phys.* **68,** 1–11 (1996).
25. Weidinger, M., Varcoe, B., Heerlein, R. & Walther, H. Trapping states in the micromaser. *Phys. Rev. Lett.* **82,** 3795–3798 (1999).
26. Brune, M. *et al.* Observing the progressive decoherence of the meter in a quantum measurement. *Phys. Rev. Lett.* **77,** 4887–4889 (1996).
27. Hagley, E. *et al.* Generation of Einstein-Podolsky-Rosen pairs of atoms. *Phys. Rev. Lett.* **79,** 1–5 (1997).
28. Maitre, X. *et al.* Quantum memory with a single photon in a cavity. *Phys. Rev. Lett.* **79,** 769–772 (1997).
29. Hulet, R. G. & Kleppner, D. Rydberg atoms in "circular" states. *Phys. Rev. Lett.* **51,** 1430–1433 (1983).
30. Nussenzveig, P. *et al.* Preparation of high principal quantum numbers "circular" states of rubidium. *Phys. Rev. A* **48,** 3991–3994 (1993).

Acknowledgements. Laboratoire Kastler Brossel is a Unité Mixte de Recherches of Ecole Normale Supérieure, Université P. et M. Curie, and Centre National de la Recherche Scientifique. This work was supported by the Commission of the European Community.

Correspondence and requests for materials should be addressed to S.H. (haroche@physique.ens.fr).

Synthesis of nuclei of the superheavy element 114 in reactions induced by ^{48}Ca

Yu. Ts. Oganessian*, A. V. Yeremin*, A. G. Popeko*, S. L. Bogomolov*, G. V. Buklanov*, M. L. Chelnokov*, V. I. Chepigin*, B. N. Gikal*, V. A. Gorshkov*, G. G. Gulbekian*, M. G. Itkis*, A. P. Kabachenko*, A. Yu. Lavrentev*, O. N. Malyshev*, J. Rohac*, R. N. Sagaidak*, S. Hofmann†, S. Saro‡, G. Giardina§ & K. Morita‖

* *Flerov Laboratory of Nuclear Reactions, JINR, 141 980 Dubna, Russia*
† *Gesellschaft für Schwerionenforschung, D-64291 Darmstadt, Germany*
‡ *Department of Physics, Comenius University, SK-84215, Bratislava, Slovakia*
§ *Dipartimento di Fisica dell'Universita di Messina, 98166 Messina, Italy*
‖ *Institute of Physical and Chemical Research (RIKEN), Wako-shi, Saitama, Japan*

The stability of heavy nuclides, which tend to decay by α-emission and spontaneous fission, is determined by the structural properties of nuclear matter. Nuclear binding energies and lifetimes increase markedly in the vicinity of closed shells of neutrons or protons (nucleons), corresponding to 'magic' numbers of nucleons; these give rise to the most stable (spherical) nuclear shapes in the ground state. For example, with a proton number of $Z = 82$ and a neutron number of $N = 126$, the nucleus ^{208}Pb is 'doubly-magic' and also exceptionally stable. The next closed neutron shell is expected at $N = 184$, leading to the prediction of an 'island of stability' of superheavy nuclei, for a broad range of isotopes with $Z = 104$ to 120 (refs 1, 2). The heaviest known nuclei have lifetimes of less than a millisecond, but nuclei near the top of the island of stability are predicted to exist for many years. (In contrast, nuclear matter consisting of about 300 nucleons with no shell structure would undergo fission within about 10^{-20} seconds.) Calculations[3–5] indicate that nuclei with $N > 168$ should already benefit from the stabilizing influence of the closed shell at $N = 184$. Here we report the synthesis of an isotope containing 114 protons and 173 neutrons, through fusion of intense beams of ^{48}Ca ions with ^{242}Pu targets. The isotope decays by α-emission with a half-life of about five seconds, providing experimental confirmation of the island of stability.

Neutron-rich nuclei with $N > 168$ can be synthesized, as we have shown earlier[6], in fusion reactions using the heaviest isotopes of uranium, plutonium and curium as targets and a ^{48}Ca ion beam. As a result of the significant mass defect of the doubly magic ^{48}Ca nucleus (magic numbers $N = 28$ and $Z = 20$), the excitation energy (E_x) of the compound nucleus at the Coulomb barrier only amounts to about 30 MeV. This corresponds to an energy $E_{lab} = 230$–235 MeV of the ^{48}Ca bombarding projectiles. The de-excitation of this nucleus should proceed mainly by the emission of three neutrons and γ-rays[7,8]. Calculations predict that the probability for the excited compound nucleus to reach the final state (evaporation residue, EVR) after the evaporation of 2 or 4 neutrons is one order of magnitude less at the bombarding ion energy near the Coulomb barrier. This circumstance should increase the survival probability of the EVRs as compared with the case of hot fusion reactions ($E_x \approx 50$ MeV), which were used for the synthesis of heavy isotopes of elements with atomic numbers $Z = 106$, 108 and 110 (refs 9–11). On the other hand, the high asymmetry of the interacting nuclei in the entrance channel ($A_p/A_T = 0.2$, $Z_p/Z_T = 1{,}880$, where A_p, A_T and Z_p, Z_T are mass and atomic numbers of the projectile and target nuclei respectively) should decrease possible dynamical limitations[12] on the fusion of massive nuclei as compared with more symmetrical cold fusion reactions.

In spite of these obvious advantages, previous attempts to synthesize new elements in ^{48}Ca-induced reactions gave only the upper limits of the production cross-sections of superheavy elements[13–15]. As is apparent now, this could be explained by the low experiment sensitivity, as the intensity of the ^{48}Ca beam was not high enough.

The first positive result was obtained in spring 1998 in the ^{48}Ca + ^{238}U reaction with a total beam dose of 3.5×10^{18} Ca ions. Two spontaneous fission events were observed, which were assigned to the decay of a new isotope of element 112 produced in the reaction ^{238}U(^{48}Ca,3n)^{283}112 with a cross-section of $\sigma_{3n} = 5^{+6}_{-3}$ picobarn (pb, 10^{-36} cm^2)[16]. The cross-section value of 1 pb corresponds to the observation of one wanted event within 4 days, providing that the beam intensity is 4×10^{12} particles per second, the number of target nuclei able to take part in the fusion reaction is 5×10^{17} and the experiment efficiency is 100%. The half-life of the new nuclide against spontaneous fission (T_{SF}), determined on the basis of the two events, was ~1.5 min. This is about 3×10^5 times longer than the α-decay half-life (T_α) of the known lighter isotope of element 112, synthesized in the reaction ^{208}Pb(^{70}Zn,1n)^{277}112 by Hofmann *et al.*[17] in 1996 (Fig. 1a).

The next experiment, performed at the end of 1998, was aimed at the synthesis of nuclei with $Z = 114$ in the reaction ^{48}Ca + ^{244}Pu. In a 34-day irradiation with a beam dose of Ca ions of 5.3×10^{18}, a decay chain—consisting of three sequential α-decays and spontaneous fission, taking about 34 min in all—was observed after the implantation of a heavy atom in the detector[18]. This decay chain may be considered as a good candidate for originating from